RESEARCH ARTICLE

WILEY

Is the soil moisture precipitation feedback enhanced by heterogeneity and dry soils? A comparative study

Maximilian Graf[1,2] | Joël Arnault[1] | Benjamin Fersch[1] | Harald Kunstmann[1,2]

[1]Institute of Meteorology and Climate Research, Karlsruhe Institute of Technology, Campus Alpin, Garmisch-Partenkirchen, Germany

[2]Institute of Geography, University of Augsburg, Augsburg, Germany

Correspondence
Maximilian Graf, Institute of Meteorology and Climate Research, Karlsruhe Institute of Technology, Campus Alpin, Garmisch-Partenkirchen, Germany.
Email: maximilian.graf@kit.edu

Abstract

The interaction between the land surface and the atmosphere is a crucial driver of atmospheric processes. Soil moisture and precipitation are key components in this feedback. Both variables are intertwined in a cycle, that is, the soil moisture – precipitation feedback for which involved processes and interactions are still discussed. In this study the soil moisture – precipitation feedback is compared for the sempiternal humid Ammer catchment in Southern Germany and for the semiarid to subhumid Sissili catchment in West Africa during the warm season, using precipitation datasets from the Climate Hazards Group InfraRed Precipitation with Station data (CHIRPS), from the German Weather Service (REGNIE) and simulation datasets from the Weather Research and Forecasting (WRF) model and the hydrologically enhanced WRF-Hydro model. WRF and WRF-Hydro differ by their representation of terrestrial water flow. With this setup we want to investigate the strength, sign and variables involved in the soil moisture – precipitation feedback for these two regions. The normalized model spread between the two simulation results shows linkages between precipitation variability and diagnostic variables surface fluxes, moisture flux convergence above the surface and convective available potential energy in both study regions. The soil moisture – precipitation feedback is evaluated with a classification of soil moisture spatial heterogeneity based on the strength of the soil moisture gradients. This allows us to assess the impact of soil moisture anomalies on surface fluxes, moisture flux convergence, convective available potential energy and precipitation. In both regions the amount of precipitation generally increases with soil moisture spatial heterogeneity. For the Ammer region the soil moisture – precipitation feedback has a weak negative sign with more rain near drier patches while it has a positive signal for the Sissili region with more rain over wetter patches. At least for the observed moderate soil moisture values and the spatial scale of the Ammer region, the spatial variability of soil moisture is more important for surface-atmosphere interactions than the actual soil moisture content. Overall, we found that soil moisture heterogeneity can greatly affect the soil moisture – precipitation feedback.

1 | INTRODUCTION

The soil moisture – precipitation feedback describes the interaction between soil moisture and precipitation and is assumed to be one of the least understood land surface – atmosphere interactions (Duerinck et al., 2016). A positive (negative) feedback describes more rain over wetter (drier) areas. Soil moisture and precipitation are two crucial variables for weather forecast and climate prediction. A better understanding of the feedback between both variables can enhance the skill of weather and climate models, as for example in medium range forecasting or drought prediction (Hao et al., 2018).

The soil moisture – precipitation feedback can be divided in direct and indirect processes. Precipitation has a direct effect on soil moisture by increasing the soil moisture content. Exceptions are very dry or saturated soils or extreme high precipitation intensities which result in increased runoff instead of increased soil moisture content (Seneviratne et al., 2010). Soil moisture also has a direct influence on precipitation by providing water through evaporation. This effect is studied under the term 'precipitation recycling' since the 1980s (Arnault et al., 2016; Eltahir & Bras, 1994; van der Ent & Savenije, 2011).

Indirectly, soil moisture influences precipitation by affecting the heating and cooling of the surface, altering turbulence, wind and convection and thus, the generation of precipitation and its distribution in time and space (Ek & Holtslag, 2004; Taylor et al., 2011). In regions where evaporation is not purely limited by either soil moisture or energy, that is, the limiting factor changing between those two factors, the uncertainty of indirect soil moisture influence is largest (Koster et al., 2004). These regions are typically located in transitional zones between wet and dry climates and sometimes referred to as the global hot spots of land surface – atmosphere interaction, including the central United States, Northern Brazil, India and large parts of West Africa among others (Koster et al., 2006; Notaro, 2008). For these regions both positive and negative soil moisture – precipitation feedback is reported.

On the one hand, higher soil moisture and evaporation can generate more precipitation, at least when precipitable water for the generation of precipitation is already available in the atmosphere (Koster et al., 2004; Seneviratne et al., 2010). This positive feedback of soil moisture and precipitation has been reported in the Great Plains (D'Odorico & Porporato, 2004; Findell & Eltahir, 1997; Su & Dickinson, 2017), Mexico (Findell et al., 2011) and West Africa (Taylor & Lebel, 1998), based on satellite and in-situ observations and model simulations.

On the other hand, several studies also characterized a negative feedback with more precipitation falling over dry soil, in relation with an interaction between convective instability, cloud formation and locally induced winds (Adler et al., 2011; Baur et al., 2018; Cook et al., 2006; Guillod et al., 2015; Kunstmann & Jung, 2007; Taylor et al., 2011, 2012).

As atmospheric processes from local boundary layer dynamics to mesoscale circulations are intertwined with each other through different scales, the soil moisture - precipitation feedback also interacts on various scales (Guillod et al., 2015). The variety of coupled processes at these scales underpin the difficulty of assessing the soil moisture – precipitation feedback (Imamovic et al., 2017; Liu et al., 2017). Kunstmann & Jung, 2007 and Yang et al., 2018 showed that a positive and a negative feedback can exist even within the same spatial and temporal scales. One of the highest uncertainties in the estimations of the soil moisture – precipitation feedback is the influence of positive or negative soil moisture anomalies on moist convection and therefore precipitation (Taylor et al., 2012). Spatial soil moisture heterogeneity was also found to have an impact on the feedback with the heterogeneity being increased through precipitation over dry soils and vice versa (Hsu et al., 2017).

Simulation datasets might be better suited than observational data sets to investigate the soil moisture – precipitation feedback, because observations are often sparse, variables may not be measurable, and the multiscale character of the feedback ranging from single thunderstorm events to continental climate may be only partially observed (Froidevaux et al. 2014). Nevertheless, observational data is still necessary to calibrate and validate simulations. Zaitchik et al. (2013) explored the soil moisture – precipitation feedback for the 2006 southern Great Plains drought by implementing a simple dynamic surface albedo scheme in the NASA Unified Weather Research and Forecasting Model (NU-WRF). They found no change in overall precipitation amount, but a positive feedback above wetter and therefore darker areas with lower albedo, which received comparatively more precipitation than brighter, drier areas during the drought. The soil moisture – precipitation feedback has been further addressed with coupled atmospheric hydrological models such as WRF-Hydro (Gochis et al., 2013). Recent studies suggest that the description of lateral terrestrial water flows in a regional climate model has an impact on surface fluxes and boundary layer dynamics, thus modifying the interaction between soil moisture and precipitation (Arnault et al., 2016, 2018; Fersch et al., 2020; Kerandi et al., 2018; Larsen et al., 2016; Maxwell et al., 2007; Rahman et al., 2015; Rummler et al., 2019; Senatore et al., 2015).

The debate about involved processes and interactions leading to either a positive or negative soil moisture – precipitation feedback is ongoing. The first objective of this study is to address this central question for two case study areas with different climatology and analyse the dependence of the feedback to soil moisture content and soil moisture heterogeneity to better understand the overall mechanism

of the soil moisture – precipitation feedback which can then help to, for example, understand and predict droughts. The first case study region is located in the prealpine, sempiternal humid region in Southern Germany and the second one in a semiarid region in West Africa, where strong surface – atmosphere interactions have been reported (Taylor et al., 2011). The second objective is to investigate the mechanisms between soil moisture and precipitation for which we evaluate several diagnostic measures of atmospheric conditions. These measures are obtained by simulation datasets from both the WRF and WRF-Hydro model systems. The two models differ by the fact that the lateral transport of water in and below the surface is neglected in WRF but considered in WRF-Hydro. This leads to differences in lateral process hydrology and in simulated soil moisture. Accordingly, a comparison between WRF and WRF-Hydro simulation allows for further insight on how soil moisture affects atmospheric variables, and hence precipitation.

2 | STUDY AREA AND DATASETS

2.1 | Study areas and observational sites

The first study area is the sempiternal humid, alpine and prealpine catchment of the Ammer river, situated in Sothern Germany covering 600 km^2. Its elevation ranges from 533 to 2300 m above sea level and features a precipitation gradient from 950 to more than 2000 mm a^{-1}. Precipitation falls year-round with a peak during the summer. An observation site of the Terrestrial Environmental Observatories (TERENO) is situated in this catchment (Kiese et al., 2018). At this site during summer months of 2015 and 2016, the ScaleX campaign in Southern Germany, took place which was the basis for a part of the here presented model results (Wolf et al., 2017). This study area is referred to as the Ammer region.

The second study area is the semiarid to subhumid catchment of the Sissili river in the West African Sudanian Savanah covering 12 800 km^2. The orography in this region is comparatively flat. The annual precipitation is around 1200 mm a^{-1} with a pronounced wet season between May and September. This study area is referred to as the Sissili region hereafter.

2.2 | Simulation datasets

The soil moisture – precipitation feedback analysis conducted in this work is based on simulation datasets obtained with WRF (Powers et al., 2017; Skamarock et al., 2005) and WRF-Hydro (Gochis et al., 2013) for the two study areas. These two models were selected to analyse the soil moisture - precipitation feedback as they have a different representation of water flow above and below the surface. WRF and WRF-Hydro share the same atmospheric and land surface model compartments. In WRF subsurface processes are described in a vertical manner only, while WRF-Hydro additionally considers the lateral routing of overland and subsurface flow of terrestrial water,

which primarily affects the spatial distribution of soil moisture. A comparison between WRF and WRF-hydro is expected to bring insight on how differences in soil moisture affect atmospheric variables in the model, including precipitation.

For the Ammer region, the WRF and WRF-Hydro datasets were provided by Fersch et al. (2020). A combination of three nested domains as shown in Figure 1 was used for the dynamic downscaling. Domain 1 covers whole Europe with a horizontal resolution of 15 km. The one-way nested domain 2 includes the Alps and their surroundings with a horizontal resolution of 3 km. The one-way nested domain 3 encompasses the Ammer region, and covers more specifically the Alpine foreland and the Alps in Bavaria (Germany) and Austria from Munich in the northeastern corner to Innsbruck in the southeastern corner, with 81 × 111 grid points and a horizontal resolution of 1 km. All three domains have 51 vertical layers with 10 hPa as the top level. The simulation period spans from mid-April to end of September 2016, with model outputs saved at an hourly interval. The first 45 days of simulation are considered as spin-up time to grant equilibrium state. Here we focus on the summer season from June to September 2016. The outer domain was initialized and forced by ERA-Interim data (Dee et al., 2011). Concerning model physics, Noah-MP was used as land surface model (Niu et al., 2011). As the soil moisture – precipitation feedback is sensitive to parametrized convection (Hohenegger et al., 2009; Taylor et al., 2013), the cumulus parametrization was activated only for the coarsest domain, while convection is explicitly resolved for domains 2 and 3 (Skamarock et al., 2005). This model setup has been run two times with WRF and WRF-Hydro, respectively. In the case of WRF-Hydro, the domains 1 and 2 are identical to the WRF case, while the terrestrial water flow routing options are activated for domain 3. The uncertainty of this model results was addressed by testing the model's sensitivity to seven land surface parameters and optimizing six of them for selected catchments with the Latin-Hypercube–One-factor-At-a-Time and Parameter Estimation and Uncertainty Analysis software. For further information regarding this model setup, calibration and results please refer to Fersch et al. (2020).

For the Sissili region the WRF and WRF-Hydro datasets were provided by Arnault et al. (2016). A combination of two domains using a one-way nesting method, as shown in Figure 2, was used. The outer domain, with a horizontal resolution of 10 km, covers a large part of West Africa and the surrounding Atlantic Ocean, while the inner domain, with 100 × 120 grid points and a horizontal resolution of 2 km, encompasses the Sissili river basin. Both inner and outer domain discretize the atmosphere into 35 vertical levels up to 20 h Pa, and the simulation period spans from January 2003 to February 2004, including a 2-month spin-up time, with model outputs saved at an hourly interval. In this paper the focus is on the rainy season from May to September 2003. Identical to the Ammer simulations, the outer domain was initialized and forced by ERA-Interim global reanalysis data, cumulus parametrization was disabled for the inner domain, and the model setup has been run two times with the WRF and WRF-Hydro models, with terrestrial water flow routing options activated only for the inner domain. The parameter runoff-infiltration
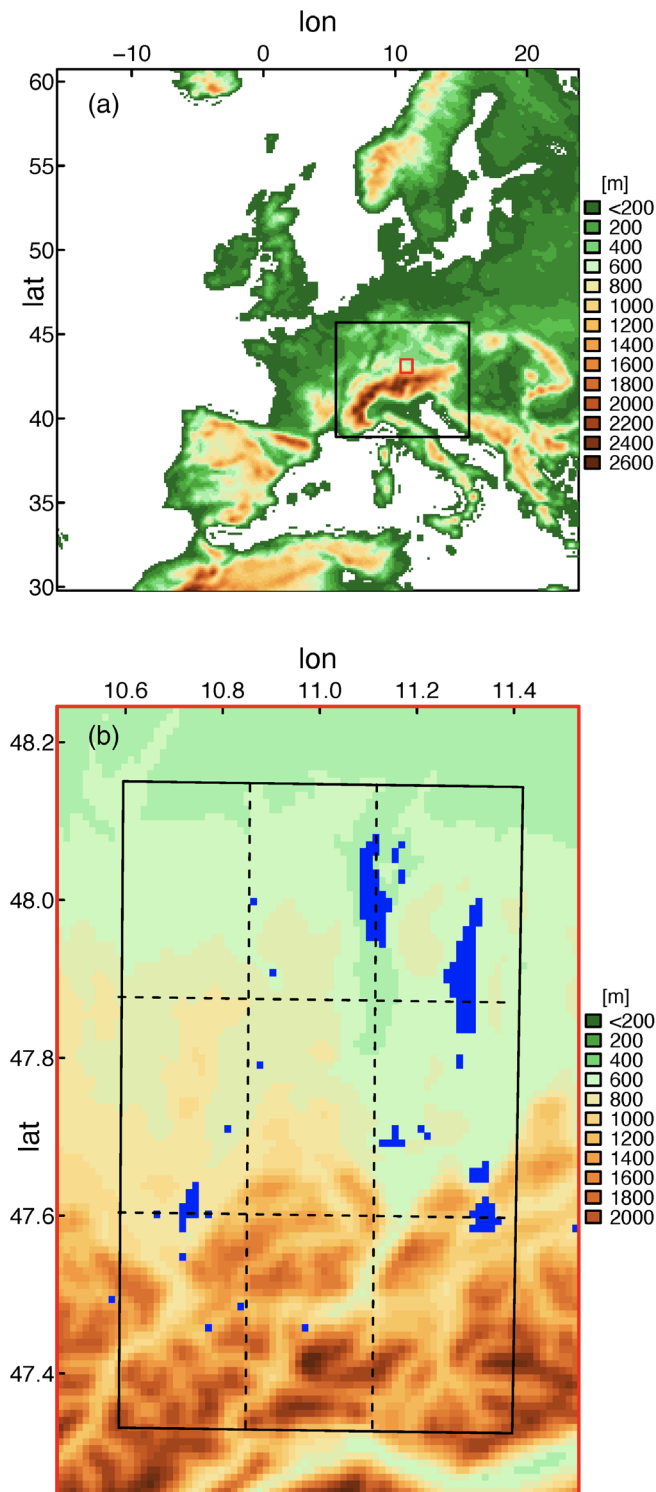
FIGURE 1 Model domains and nesting configuration for the Ammer region. Model domains of the whole model chain in (a). The inner domain 3 is framed red in both plots. The area used for analysis is framed black in the lower plot in (b). Lakes are blue

FIGURE 2 Model domains and nesting configuration for the Sissili region. Model domains of the whole model chain in (a). The inner domain 2 is framed red in both plots. The area used for analysis is framed black in the lower plot in (b). Lakes are blue

For further information regarding this model setup, its calibration and results please refer to Arnault et al. (2016).

In the following, the above-described WRF and WRF-Hydro simulation datasets are used to investigate the soil moisture – precipitation feedback mechanisms occurring in both the Ammer and Sissili regions.

2.3 | Observational datasets

The accuracy of model results is evaluated using observed precipitation. In case of the Ammer region, we use the "REGNIE" data product, which is an hourly gauge-based product provided by the German

partitioning was selected for a sensitivity analysis to estimate the uncertainty and calibrate it for both the inner and out domain of this model setup. The impact was found to be higher on the outer domain.
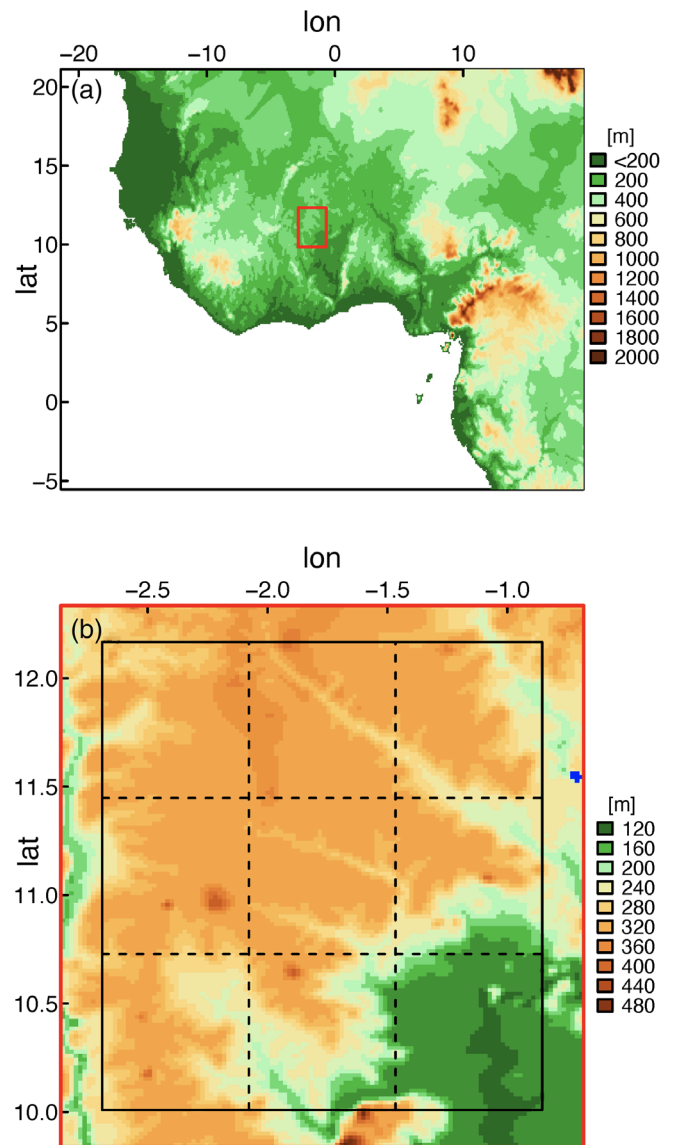
Weather service. This dataset has a daily temporal resolution and is regionalized into a raster with 1 km grid size (Rauthe et al., 2013). In the case of the Sissili region, we use the daily product from the quasi-global CHIRPSv2.0 dataset (Funk et al., 2015). CHIRPSv2.0 has a spatial resolution of 0.05° and is based on satellite based Cold Cloud Duration observations which are merged with rain gauge information from a variety of public and private data archives as well as from national meteorological agencies.

3 | METHODS

As soil moisture potentially affects precipitation through boundary layer dynamical processes, we focus our analysis on the link between soil moisture, surface fluxes, moisture flux convergence above the surface (SMFC), convective available potential energy (CAPE) and precipitation. The link between soil moisture and precipitation is more particularly assessed with the normalized model spread and a soil moisture heterogeneity measure, as detailed in the following sections.

3.1 | Moisture flux convergence above the surface (SMFC) and convective available potential energy (CAPE)

Both SMFC and CAPE are used to describe the state of the atmosphere and their role in the soil moisture – precipitation feedback is analysed.

The transport of moisture in the atmosphere, a crucial factor for the generation, location and intensity of precipitation is described by the moisture flux convergence above the surface (SMFC). This measure was used in different studies since the 1950s to estimate large scale precipitation (Bradbury, 1957; Wei et al., 2016), cloud coverage in the tropics (Krishnamurti, 1968), convective initiation and severe weather (Petersen & Petersen, 2000; van Zomeren & van Delden, 2007). Here SMFC is calculated with code from the NCAR Command Language (NCL) in the lowest atmospheric level using humidity q and the wind vectors u and v of the model simulations. SMFC is used to investigate the relation between soil moisture and this atmospheric variable on the initiation of moist convection via

$$SMFC = -u\frac{\partial q}{\partial x} - v\frac{\partial q}{\partial y} - q\left(\frac{\partial u}{\partial x} + \frac{\partial v}{\partial y}\right) \quad (1)$$

The vertically integrated variable CAPE characterizes the stability of the atmosphere (Rahman et al., 2015). It describes the buoyant energy integrated from the equilibrium level (Z_{EL}) to the level of free convection (Z_{LFC}) of an idealized air parcel (Yin et al., 2015)

$$CAPE = g * \int_{Z_{EL}}^{Z_{LFC}} \left(\frac{T_v - T_e}{T_e}\right) dz \quad (2)$$

Code from NCL is used to calculate CAPE from model output, where g is the gravitational acceleration, T_v the virtual temperature of the maximum

theta-e parcel in the lowest 3 km of the atmosphere and T_e the virtual temperature of the environment (Doswell & Rasmussen, 1994).

The evolution of convective precipitation and severe weather is strongly related to CAPE, hence it is often used in the forecast and analysis of those events (Gartzke et al., 2017; Riemann-Campe et al., 2009). High values of CAPE are often found during deep (moist) convection and it is also used as a proxy to distinguish synoptic and convective forced precipitation (Gartzke et al., 2017).

The vertical integration of this measure differentiates it from other inspected variables, for example, sensible heat flux. It allows presumptions not only for effects of surface – atmosphere interaction near the surface, but also for the impact on the atmospheric boundary layer. More specifically, the ratio between CAPE and precipitation allows the computation of a convective adjustment time scale τ, which quantifies the relative influence of synoptic processes and local effects on a weather situation (Done et al., 2006; Keil & Craig, 2011).

3.2 | Normalized model spread

The simulations of section 2.2 have been designed so that the WRF and WRF-Hydro inner domains for each study region are forced by the same atmospheric boundary condition. This is to prevent large-scale atmospheric variability to affect the inner domain results, and ensures that the differences between the WRF and WRF-Hydro simulated atmosphere are mainly triggered by differences in soil moisture (Rummler et al., 2019).

The difference between WRF and WRF-Hydro simulation results is evaluated with the normalized model spread S of hourly variables

$$S = \frac{1}{m}\sqrt{(WRF - m)^2 + (WRF_{hy} - m)^2} \quad (3)$$

with

$$m = 0.5(WRF + WRF_{hy}) \quad (4)$$

S is the ratio between the root of the mean squared error and the model mean m. This normalized measure is decoupled from the magnitude of the numerical value and enables an independent comparison of model results. The abbreviations WRF and WRF_{hy} in (3) and (4) represent the considered variables in this study, namely precipitation, sensible heat flux, evaporation, CAPE and SMFC from the respective model. All variables are convolved by a 21 km Gaussian filter before the calculation of m and S. The convolution allows the characterization of the convective-scale environment without losing too much spatial information (Keil et al., 2014). In order to focus on cloud convection events, only the convolved grid-cells corresponding to daily maxima of convective adjustment time scale exceeding 3 h with an hourly precipitation rate exceeding 1 mmh^{-1} are considered (Arnault et al., 2018; Kühnlein et al., 2014). These events are hereafter called maximum τ events.

3.3 | Classification of the soil moisture spatial heterogeneity

Soil moisture patterns can be described as a function of the mean soil moisture (Korres et al., 2015). To illustrate the influence of soil moisture on surface atmosphere interactions and atmospheric variables, the behaviour of these variables above soil moisture patterns is assessed. Here the soil moisture patterns are expressed through the spatial gradient of soil moisture ∇S, a measure of surface heterogeneity which potentially influences cloud convection (Clark et al., 2004). ∇S is calculated in x and y direction for the uppermost soil level of the model output. Each soil moisture gradient time slice of the model data is smoothed by a Gaussian filter with a kernel size of 21 km in order to characterize surface atmosphere interactions at the convective-scale. Each resulting time slice is split up into 10 percentiles representing ∇S classes from low to high gradients, allowing for quantile-wise inspection of the result.

For the area of each ∇S class in time step n, the mean of surface and atmospheric variables is calculated for the timestep $n + 1$ so that ∇S characterizes the state of the land surface before the occurrence of precipitation. All resulting values are aggregated into averages for each ∇S class per hour of the day. This allows for a detailed investigation of the soil moisture's influence on land-atmosphere exchange processes initiating and modulating precipitation in a spatio-temporal manner. In particular for each ∇S class, the energy exchanges between the surface and the atmosphere are quantified with averaged sensible heat flux and evaporation, the atmospheric conditions with averaged SMFC and CAPE, and the soil moisture – precipitation feedback with averaged soil moisture content and precipitation.

4 | RESULTS

4.1 | Evaluation of simulated precipitation and soil moisture

Precipitation results of both models are validated against observational precipitation datasets and the soil moisture content of the uppermost soil layer (0–0.1 m) of both models are compared in Figure 3 for the Ammer region and in Figure 4 for the Sissili region. We restricted the analysis to this layer because it responds fast to variations of the overlaying atmospheric conditions whereas the deeper layers are rather relevant for processes on longer time scales.

For the Ammer region a difference in soil moisture content of about 0.03–0.05 $m^3 m^{-3}$ is found between WRF and WRF-Hydro. This difference is in the range of 10–20% of the typical yearly variation. Both models show little differences in the precipitation (not visible in Figure 3) in this region even though the soil moisture differences between both simulations can be quite large. On a daily and hourly basis, larger differences of timing and place of precipitation can be found between both model realizations. Compared to the observational product REGNIE, the cumulative sum of both model realizations and REGNIE is similar.
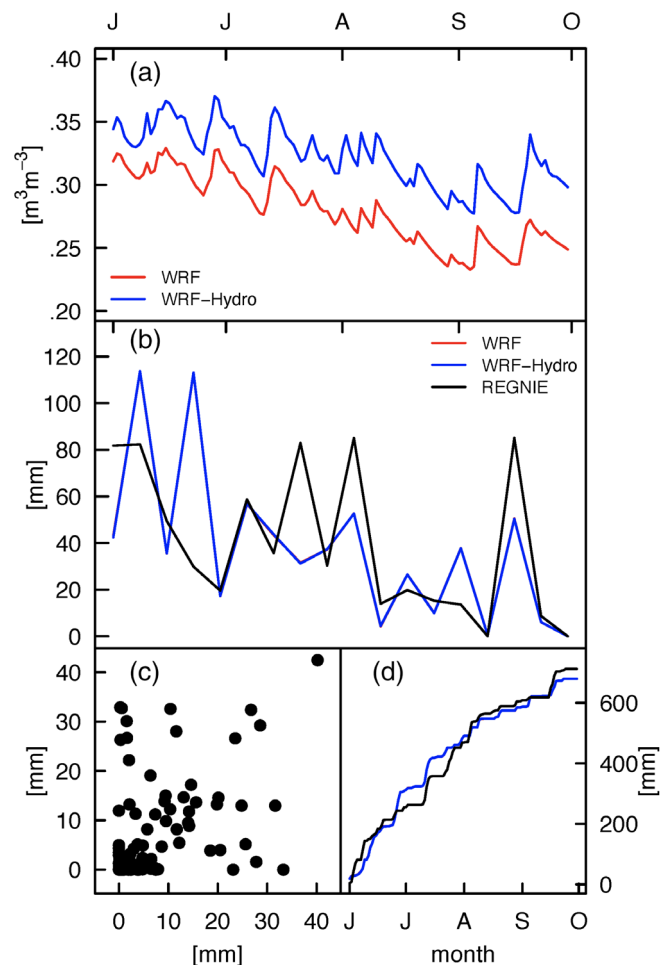

FIGURE 3 Area mean soil moisture of WRF and WRF-hydro for the Ammer region in (a). Area mean precipitation of both models compared to REGNIE as (b) weekly sum, (c) scatterplot of daily WRF-hydro and REGNIE precipitation and (d) cumulative precipitation

For the Sissili region the soil moisture is almost on the same level in both simulations, while the precipitation differs more than in the Ammer region. The modelled precipitation exceeds the CHIRPSv2.0 precipitation by a third in the analysed five-month period, but the onset of the rainy season and its course is recreated quite well. The intra-seasonal discrepancy of modelled and observed data is also visible in the scatterplot.

4.2 | Normalized spread of precipitation versus normalized spread of other variables

The normalized spread between WRF and WRF-Hydro shows where the two different boundary conditions of the soil moisture description cause a distinguishable difference for the considered variables sensible heat flux, evaporation, SMFC, CAPE, and precipitation. With low synoptic forcing the influence of exchange processes between the surface and the atmosphere is favoured and the variable spreads can reach higher values. Contrarily, large scale formations like cyclones do
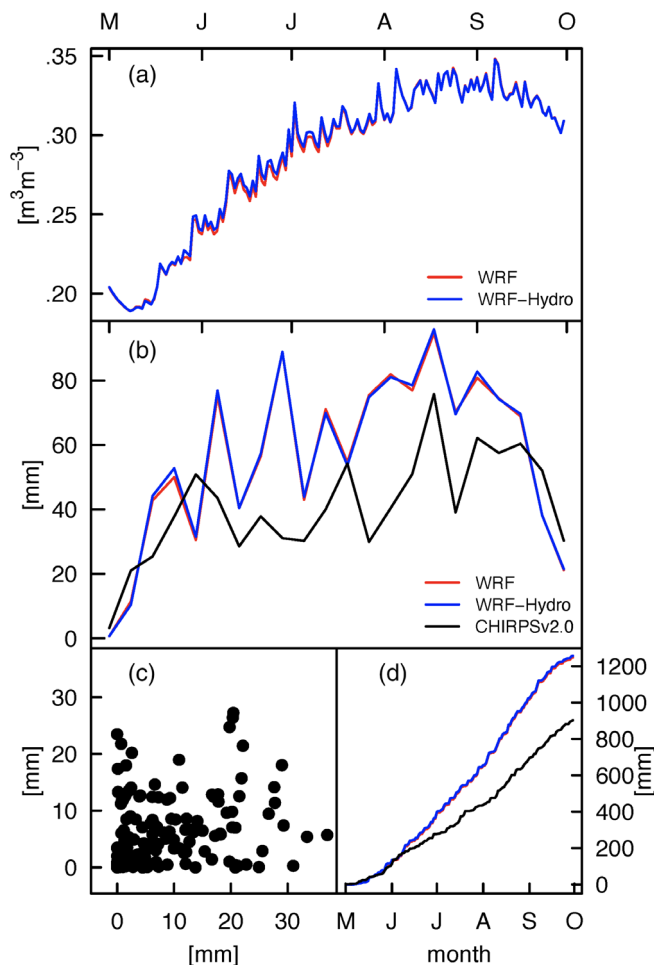
FIGURE 4 Area mean soil moisture of WRF and WRF-hydro for the Sissili region in (a). Area mean precipitation of both models compared to CHIRPSv2.0 as (b) weekly sum, (c) scatterplot of daily WRF-hydro and CHIRPSv2 precipitation and d) cumulative precipitation

not result in high spreads due to strong forcing at the atmospheric boundaries of the analysed model domain.

The relationship between the spread of precipitation ($S_{precipitation}$) and the spread of sensible heat flux, evaporation, CAPE and SMFC is shown in Figure 5 for the Ammer region and in Figure 6 for the Sissili region, both for an hourly resolution.

In the Ammer region the sensible heat flux and evaporation spreads show a weak dependence to $S_{precipitation}$ with low values of r^2. A cluster with highest $S_{sensible\_heat\_flux}$ values and almost no precipitation spread is found. It can be explained by high precipitation amounts due to strong synoptic forcing with minimal spread in precipitation. S_{CAPE} and S_{SMFC} do not show this clustering and the low precipitation spread indicates strong influence of the atmospheric boundary and weak influence of the surface boundary, thus, S_{CAPE} and S_{SMFC}, both yield higher r^2.

$S_{sensible\_heat\_flux}$ shows higher r^2 at the daily maximum of τ, plotted in red. Albeit the correlation is low, the above-mentioned cluster is almost completely excluded in this case, due to the fact that high τ

values depend on high CAPE values. Similar to results from other studies (Arnault et al., 2018; Keil et al., 2014), τ provides a good estimate of situations with low synoptic forcing. S_{CAPE} and S_{SMFC} show almost no change in r^2 when only the highest τ values are considered, because they are already filtered from high synoptic forcing. Despite that, highest values of spreads are excluded when the highest τ values are considered, as τ decreases with the removal of CAPE at the onset of precipitation.

The Sissili data shows highest correlation for $S_{sensible\_heat\_flux}$ and no correlation for S_{CAPE}. Another difference with the Ammer region is the distribution of $S_{precipitation}$ which almost reaches the maximal possible spread value of $\sqrt{2}$ in West Africa. Only the relationship between $S_{precipitation}$ and $S_{sensible\_heat\_flux}$ is higher for the maximum τ events. S_{SMFC} tends to be higher for maximum τ events while showing a weaker correlation. When only the highest τ values are considered, the correlation values are thereby in the same range as for the Ammer region, while S_{CAPE} shows no correlation.

4.3 | Soil moisture pattern

Soil moisture patterns described by convolved soil moisture gradients are used to assess the influence of soil moisture anomalies on surface and atmospheric variables for both study regions. The diurnal cycle of surface and atmospheric variables and their dependency to ∇S classes (quantiles) are examined in Figures 7 and 8 for the WRF-Hydro simulations and in Figures 9 and 10 for the WRF simulations. Additionally, the behaviour of mean soil moisture and precipitation is shown in these figures. The overall distribution of soil moisture and ∇S is similar for both WRF and WRF-Hydro in both regions, with a slightly higher variability of soil moisture in WRF-Hydro and higher soil moisture values for the Ammer catchment.

For both regions, variables show a distinct diurnal cycle, except for soil moisture. For sensible heat flux, evaporation and CAPE the magnitude of the diurnal cycle exceeds the differences between ∇S classes in both regions of interest. Sensible heat flux and evaporation have their maximum at noon when incoming radiation is at its maximum. ∇S ranges from almost negligible values in both regions in class one up to 0.003 m^3 m^{-3} (Ammer) and 0.0015 m3 m^{-3} (Sissili) in class 10. These values correspond to an average change of soil moisture content of about 1% per km in both cases.

In the Ammer region, the corresponding soil moisture values are similarly high for low and medium gradients and drop to lower values at highest ∇S classes. Daytime values are characterized by a higher sensible heat flux and lower evaporation over higher moisture gradient classes with lower soil moisture. With less available moisture, the partitioning between sensible and latent heat leans more to the sensible heat flux. This affects the atmosphere which can be seen in SMFC and CAPE.

SMFC shows the strongest dependence to ∇S among all analysed variables. The amplitude of SMFC variations with respect to ∇S even exceeds the diurnal cycle in this case. Highest SMFC values can be
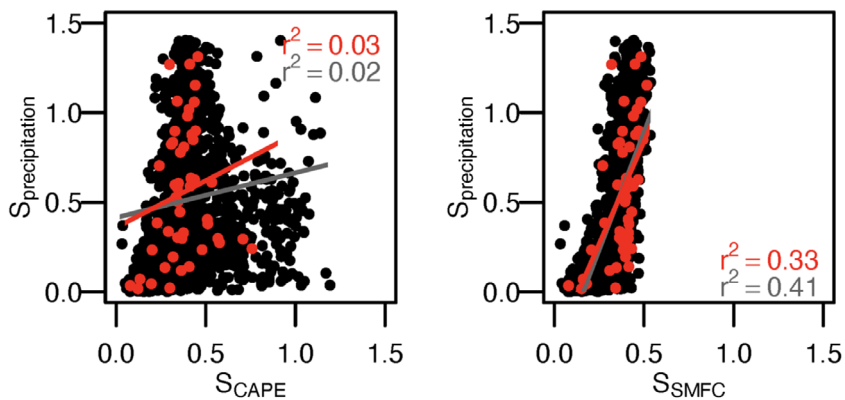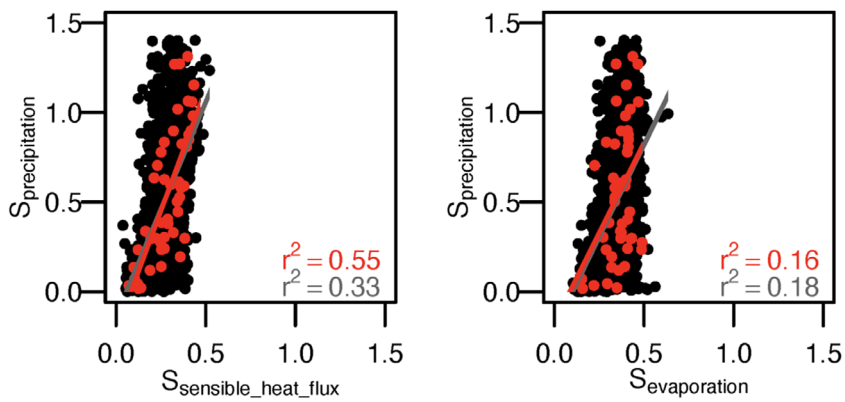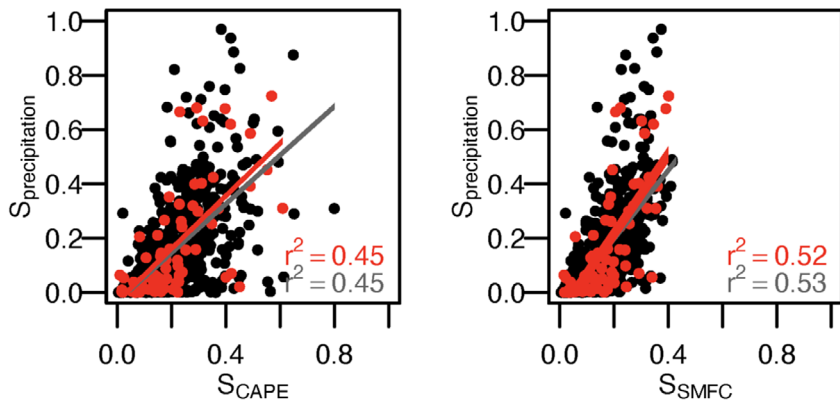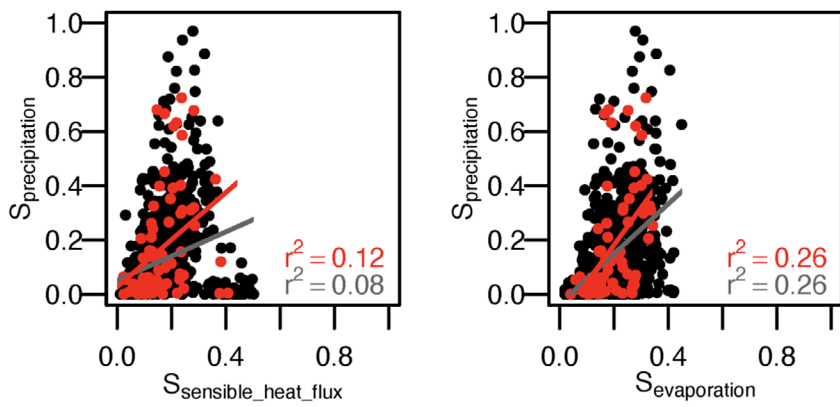
FIGURE 5 Scatter plot of the normalized hourly spread of sensible heat flux, evaporation, CAPE and SMFC against the normalized spread of precipitation for the Ammer region. Hourly spread values for the times when the convective time scale τ is at its maximum are highlighted in red. Linear regression for both datasets with values of r^2 are drawn by the black and red line respectively

FIGURE 6 Scatter plot of the normalized hourly spread of sensible heat flux, evaporation, CAPE and SMFC against the normalized spread of precipitation for the Sissili region. Hourly spread values for the times when the convective time scale τ is at its maximum are highlighted in red. Linear regression for both datasets with values of r^2 are drawn by the black and red line respectively
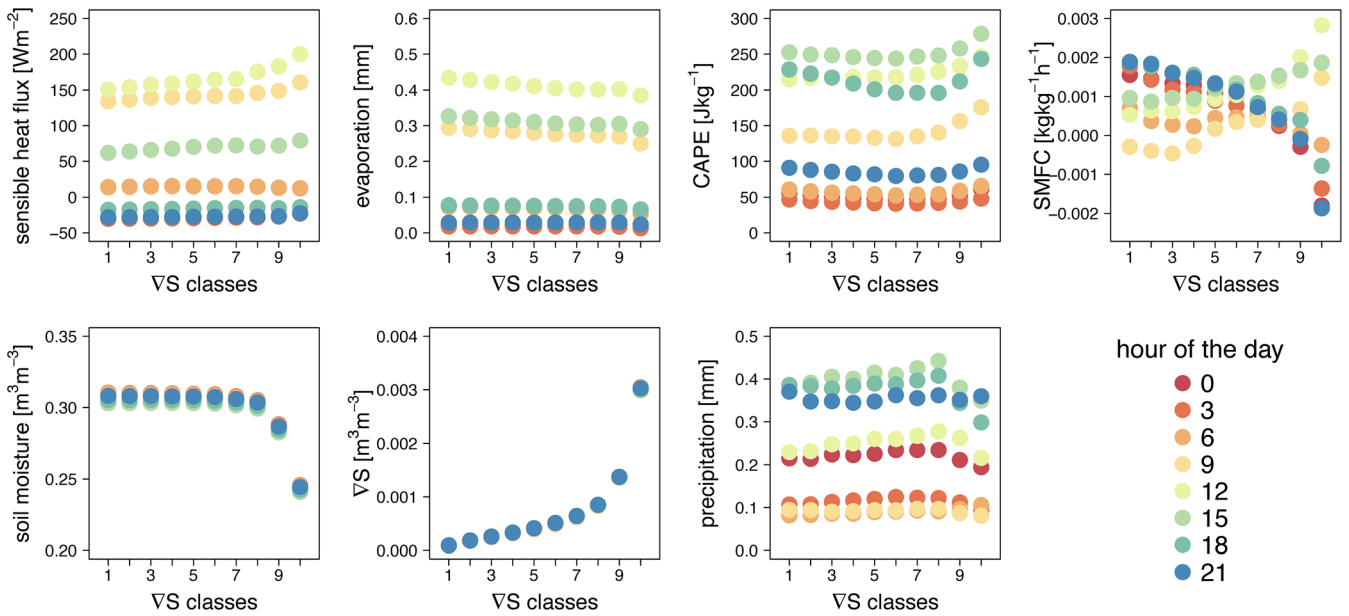
FIGURE 7 Diurnal behaviour of sensible heat flux, evaporation flux, CAPE, SMFC, soil moisture, soil moisture gradient norm and precipitation according to soil moisture gradient classes ∇S for the Ammer region and for the period from June to September 2016, from the WRF-hydro simulation
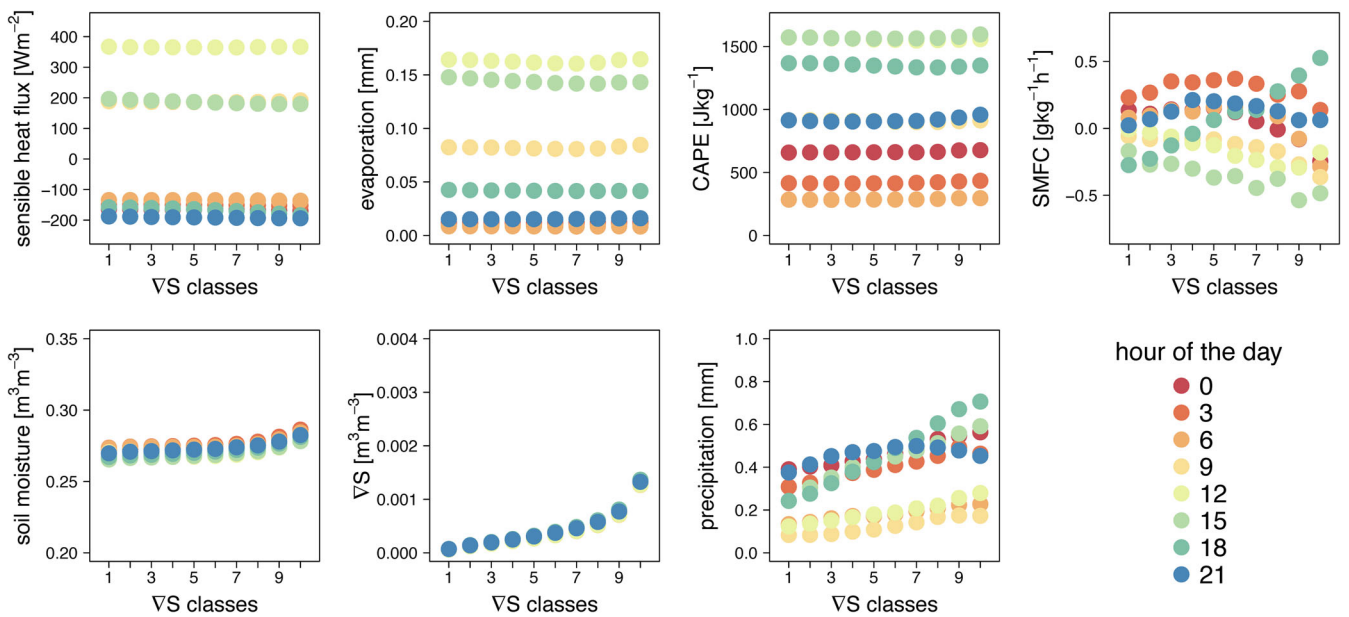

FIGURE 8 Diurnal behaviour of sensible heat flux, evaporation flux, CAPE, SMFC, soil moisture, soil moisture gradient norm and precipitation according to soil moisture gradient classes ∇S for the Sissili region and for the period from May to September 2003, from the WRF-hydro simulation

found over high ∇S classes during daytime, and over low ∇S classes during nighttime.

CAPE reaches its maximum in the afternoon, being built up from early morning hours. At 9 and 12 UTC the generation of CAPE occurs faster over regions with a higher soil moisture gradient, which indicates favourable conditions for the initation of convection. Similar results were found in idealized model studies (Baur et al., 2018; Rieck

et al., 2014). Highest values are found at 15 UTC over the highest ∇S class. In the evening CAPE declines fastest over medium to high ∇S classes, down to relatively low values overnight. The differences between WRF (Figure 9) and WRF-Hydro (Figure 10) in the Ammer region for CAPE and SMFC depend on the differences in the soil moisture content. In WRF-Hydro, CAPE and SMFC display more variability and CAPE reaches higher maxima. This can be attributed to
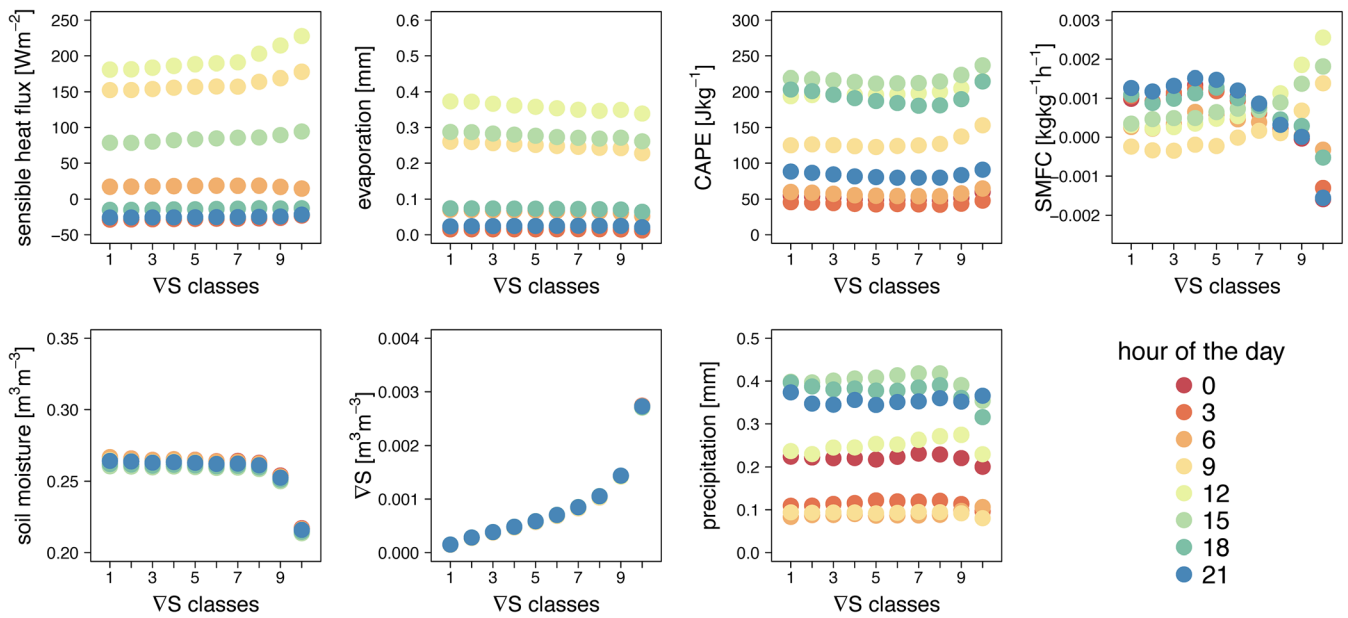
FIGURE 9 Diurnal behaviour of sensible heat flux, evaporation flux, CAPE, SMFC, soil moisture, soil moisture gradient norm and precipitation according to soil moisture gradient classes ∇S for the Ammer region and for the period from June to September 2016, from the WRF simulation
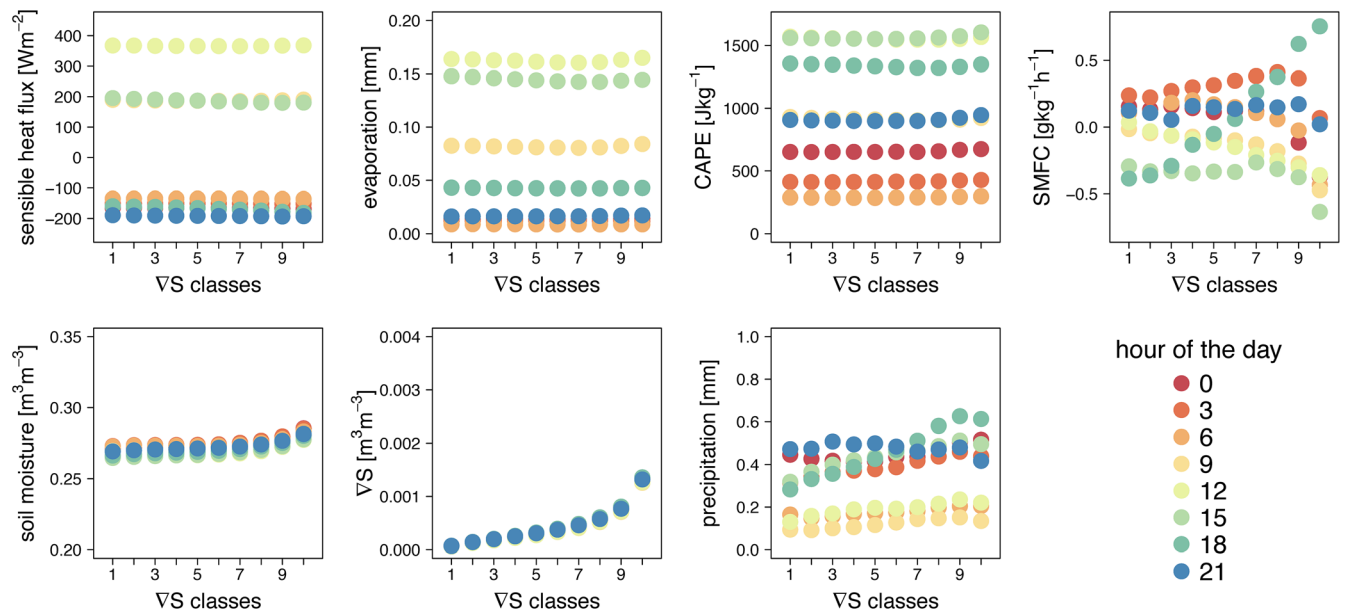

FIGURE 10 Diurnal behaviour of sensible heat flux, evaporation flux, CAPE, SMFC, soil moisture, soil moisture gradient norm and precipitation according to soil moisture gradient classes ∇S for the Sissili region and for the period from May to September 2003, from the WRF simulation

higher soil moisture variability and slightly higher contrasts of soil moisture gradients in WRF-Hydro. Intuitively, in areas with high convergence of moisture and high CAPE, more precipitation is expected. Precipitation's result in Figure 7 confirms this behaviour for all ∇S classes except for the two highest classes in the Ammer region, where it decreases.

With less pronounced soil moisture gradients in Sissili, the soil moisture values in the ∇S classes are less differentiated. Contrarily to

the Ammer region, soil moisture values in Sissili rise at highest ∇S classes, because wet spots are the exception in this dry region and produce the highest gradient in this area. For the Sissili region fewer variables seem to be affected by the gradient of soil moisture. For sensible heat flux, evaporation, and CAPE there are little variations in mean values over ∇S classes. SMFC shows mean positive values over areas with higher ∇S only in the afternoon. The strongest relation with ∇S is found for precipitation with the largest amounts over

highest ∇S classes. This distribution over ∇S is largest during the afternoon. In comparison to WRF-Hydro, the WRF simulation has a minimal lower average soil moisture content which results in almost identical patterns of sensible heat flux, evaporation, CAPE, and ∇S.

5 | DISCUSSION

5.1 | Normalized spreads

With the normalized spread between WRF and WRF-Hydro, precipitation events during low synoptic forcing situations are highlighted. The normalized spreads of CAPE and SMFC show similar behaviour with respect to the normalized spread of precipitation in the Ammer region while in the Sissili region the normalized spread of CAPE shows no correlation and seems to be not a main factor for the generation of precipitation spread. Sensible heat flux and evaporation are not directly linked to precipitation, but still can have an influence on the buildup of CAPE. $S_{precipitation}$ is only calculated during precipitation events, which therefore can affect the spread of sensible heat flux and evaporation after the onset of precipitation. The dependence between $S_{precipitation}$ and $S_{sensible\_heat\_flux}$ is larger when τ reaches its maximum at the onset of precipitation for both the Ammer and the Sissili region. For both regions, maxima in the spread of precipitation and other variables may not occur at the precipitation onset when τ is maximum. Indeed, the precipitation spread may build up gradually, thus influencing the spread of the other variables which in turn can lead to an enhanced precipitation spread and result in a maximum $S_{precipitation}$ after the daily maximum of τ.

5.2 | Soil moisture pattern

The relatively small values of ∇S in both regions can be explained by the Gaussian filtering process convolving the soil moisture field and also by the averaging over all days. This effect is greater on the 2 km grid size of the Sissili domain than on the 1 km grid size of the Ammer domain. Nevertheless, a distinguishable set of soil moisture gradient classes could be produced for both cases. Another reason for small ∇S values in both domains could be the detailed orographic features in the used resolutions. According to Imamovic et al. (2017) orographic energy can reduce the strength of the local soil moisture – precipitation feedback.

For all simulations and both regions, areas with higher ∇S are more prone to be areas of convective initiation. Soils are typically drier and soil moisture is more heterogenous when it has not been raining for a longer period which often can be the case when convection occurs and synoptic forcing is weak. With the highest ∇S values found at the driest areas of the domain, the initiation of precipitation is more likely linked to these dry areas in the Ammer region. It is acknowledged that background wind (Froidevaux et al., 2014) and orography (Imamovic et al., 2017) can also have an influence on precipitation location. Even in an idealized case the convergence of moist

air over soil moisture gradients can lead to a displacement of the precipitation due to different pressure caused by soil moisture gradients (Baur et al., 2018). In the case of the Ammer region, the highest precipitation over the third highest ∇S class suggests that rain falls nearby the driest spots when the soil moisture gradient is still high but moderated by relatively high mean soil moisture values. This leads to the conclusion, that at least for the observed moderate soil moisture values and the spatial scale of the Ammer region, the spatial variability of soil moisture is more important for surface-atmosphere interactions than the actual soil moisture content.

The differentiation along ∇S especially for SMFC and precipitation suggests that the soil moisture – precipitation feedback is enhanced over areas with higher soil moisture gradients in both study regions. For the Ammer region the soil moisture – precipitation feedback has a weak negative sign while it has a positive signal for the Sissili region.

The result for the Ammer catchment compares well to the negative feedback found for the nearby low mountain range of the Black Forest (Barthlott & Kalthoff, 2011) and for a more complex alpine region (Hohenegger et al., 2009). Both studies used an explicit convection scheme and a similar resolution (2.2 and 2.8 km) while (Hohenegger et al., 2009) also analysed a 25 km simulation with a parameterized convection scheme which resulted in a positive feedback. Leutwyler et al. (2021) also compared explicit and parameterized convection. While these authors found an overall positive feedback driven by CAPE for both cases contrasting our study, they also concluded that spatial soil moisture gradients were the main driver for precipitation during negative feedback episodes.

Seneviratne et al. (2010) concluded that the main objective in understanding soil moisture – precipitation feedback is the influence of soil moisture on the generation of precipitation, which according to our result can be assigned to areas with high soil moisture gradients and lower soil moisture values in the Ammer region, and areas with higher soil moisture values in the Sissili region.

5.3 | Benefits and limitations of coupled modelling on the soil moisture – precipitation feedback

The assessment of the soil moisture – precipitation feedback in this study was conducted using the modelling framework WRF and WRF-Hydro. The major advantage of such models over observational data sets is the continuity and availability of all relevant variables. A common drawback of such earth system models is their approximation of physical processes. Parameterizations are often used to represent the real-world processes, thus simplifying or neglecting physical principals. The coupling of the atmospheric and hydrologic compartments contributes to improve the model's realism at their interface.

Another limitation is the internal variation of model variables which increases the uncertainty of the model results. Because the individual model runs which are analysed in this study are internally physically consistent, it is assumed that the interaction between the variables considered in this study is also consistent. Additionally, this

study analyses the feedback within a single model realization, and the feedback occurring at a particular time is not addressed.

Nevertheless, observational data sets are and will be as important as models to study the earth system. Santanello et al. (2018) proposed to continuously observe the lower troposphere and particularly the important variables for land surface – atmosphere coupling. Such observations are not only necessary to calibrate and validate model results, especially in the context of the soil moisture - precipitation feedback, but also to test the transferability of model study results from a regional scale like in this study to global scale.

6 | CONCLUSION

The feedback loop between soil moisture and precipitation and its mechanisms depend on many factors while its implications for understanding and predicting the earth system are fundamental. Here this feedback was analysed for two climatologically different regions. The influence of soil moisture on surface fluxes, SMFC, CAPE and precipitation was quantified. A two-model comparison, namely with WRF and WRF-Hydro, using fixed atmospheric boundary conditions with a different description of lateral water flow, was used for the two regions situated in Southern Germany (Ammer catchment) and West Africa (Sissili catchment).

For both regions the two models produced reasonable precipitation time series. Soil moisture differences in the Ammer region were found to be relatively large while precipitation differences between both models were relatively small. In the case of the Sissili, the soil moisture time series were on average more similar while the precipitation differences were larger.

The normalized spread of precipitation between both models in the Ammer and Sissili region increased with enhanced spatial variability of surface fluxes and of variables describing atmospheric stability.

When examined in detail, single variables showed a distinct behaviour over different soil moisture gradient classes. The major influence of the soil moisture gradient on the partitioning of sensible and latent heat could be shown for the Ammer region. In this prealpine, sempiternal humid region, the partitioning of sensible and latent heat also modulated SMFC and the buildup of CAPE, both closely linked to the initiation of moist convection and precipitation. Precipitation followed the soil moisture gradient to a certain point, but did not fall at the same location. The areas with the highest precipitation amounts did not match the areas with the highest soil moisture gradients. For the semiarid to subhumid Sissili region there was no difference of the partitioning between sensible heat flux and evaporation for different soil moisture gradient classes. SMFC showed again a higher dependence to soil moisture gradient classes, and so did the precipitation, which supported a higher probability for precipitation over areas with higher contrast / higher soil moisture gradient when it was drier in the case of the Sissili.

In summary, the generation of moist convection is favoured over surfaces with moderately high soil moisture gradients in the Ammer region, while for the Sissili region the location of precipitation tends to be related to areas with high soil moisture gradients. For moderately saturated soils of the Ammer region as well as for the drier soils of the Sissili region, not only the soil moisture content but also the gradient of soil moisture over an area is affecting the spatial distribution of the generation of convection and precipitation.

The heterogeneity of soil moisture matters and therefore should be considered when investigating the feedbacks at the surface – atmosphere boundary. This finding from the regional scale can also be placed in the global context of earth system models (ESM). Clark et al. (2015) concluded that the poor representation of many hydrological processes in land ESM directly leads to limitations in their ability to represent land surface – atmosphere interactions. In this study we show that an improved representation of later al water flow changes the separation of surface fluxes, atmospheric variables and precipitation. The evaluation of such earth system model behaviour can benefit from global high resolution observation of soil moisture, cloud and precipitation from remote sensing (Santanello et al., 2018). Also, a better understanding of the diurnal pattern of variables influenced by the soil moisture – precipitation feedback can potentially lead to an improvement of short-term forecasts (Santanello et al., 2016).

From a global perspective for the global hotspots of land surface – atmosphere interaction, like the West African savanna region studied here, the soil moisture – precipitation feedback has an impact on whether a year becomes drier or wetter. This in turn can decide if the region acts as a carbon sink or source in this respective year (Gentine et al., 2019).

An interesting question for future research would be how the change of spatial model resolution, both in regional and global earth system models would influence the soil moisture heterogeneity and thus the feedback mechanism. CAPE and SMFC, which were used as valuable variables to assess the linkage between the surface and the atmosphere, and their use can be recommended for future research.

Overall, we cannot fully conclude whether precipitation accumulates more over the drier or wetter patches at the sempiternal humid Ammer catchment, but in the case of the semiarid to subhumid Sissili catchment precipitation tends to fall over wetter patches, which emphasizes a positive soil moisture – precipitation feedback.

(http://chg.geog.ucsb.edu/data/chirps) as well as the usage of the REGNIE data from the German Meteorological Service (https://www.dwd.de/DE/leistungen/regnie/regnie.html).

ORCID

Maximilian Graf https://orcid.org/0000-0003-2246-1273
Joël Arnault https://orcid.org/0000-0001-8859-5173
Benjamin Fersch https://orcid.org/0000-0002-4660-1165
Harald Kunstmann https://orcid.org/0000-0001-9573-1743

REFERENCES

Adler, B., Kalthoff, N., & Gantner, L. (2011). The impact of soil moisture inhomogeneities on the modification of a mesoscale convective system: An idealised model study. *Atmospheric Research*, 101(1), 354–372. https://doi.org/10.1016/j.atmosres.2011.03.013

Arnault, J., Rummler, T., Baur, F., Lerch, S., Wagner, S., Fersch, B., Zhang, Z., Kerandi, N., Keil, C., & Kunstmann, H. (2018). Precipitation sensitivity to the uncertainty of terrestrial water flow in WRF-hydro: An ensemble analysis for Central Europe. *Journal of Hydrometeorology*, 19(6), 1007–1025. https://doi.org/10.1175/JHM-D-17-0042.1

Arnault, J., Wagner, S., Rummler, T., Fersch, B., Bliefernicht, J., Andresen, S., & Kunstmann, H. (2016). Role of runoff–infiltration partitioning and resolved overland flow on land–atmosphere feedbacks: A case study with the WRF-hydro coupled modeling system for West Africa. *Journal of Hydrometeorology*, 17(5), 1489–1516. https://doi.org/10.1175/JHM-D-15-0089.1

Barthlott, C., & Kalthoff, N. (2011). A numerical sensitivity study on the impact of soil moisture on convection-related parameters and convective precipitation over complex terrain. *Journal of the Atmospheric Sciences*, 68(12), 2971–2987. https://doi.org/10.1175/JAS-D-11-027.1

Baur, F., Keil, C., & Craig, G. C. (2018). Soil moisture–precipitation coupling over Central Europe: Interactions between surface anomalies at different scales and the dynamical implication. *Quarterly Journal of the Royal Meteorological Society*, 144(717), 2863–2875. https://doi.org/10.1002/qj.3415

Bradbury, D. L. (1957). Moisture analysis and water budget in three different types of storms. *Journal of Meteorology*, 14(6), 559–565. https://doi.org/10.1175/1520-0469(1957)014<0559:MAAWBI>2.0.CO;2

Clark, D. B., Taylor, C. M., & Thorpe, A. J. (2004). Feedback between the land surface and rainfall at convective length scales. *Journal of Hydrometeorology*, 5(4), 625–639. https://doi.org/10.1175/1525-7541(2004)005<0625:FBTLSA>2.0.CO;2

Clark, M. P., Fan, Y., Lawrence, D. M., Adam, J. C., Bolster, D., Gochis, D. J., Hooper, R. P., Kumar, M., Leung, L. R., Mackay, D. S., Maxwell, R. M., Shen, C., Swenson, S. C., & Zeng, X. (2015). Improving the representation of hydrologic processes in earth system models. *Water Resources Research*, 51(8), 5929–5956. https://doi.org/10.1002/2015WR017096

Cook, B. I., Bonan, G. B., & Levis, S. (2006). Soil moisture feedbacks to precipitation in southern Africa. *Journal of Climate*, 19(17), 4198–4206. https://doi.org/10.1175/JCLI3856.1

Dee, D. P., Uppala, S. M., Simmons, A. J., Berrisford, P., Poli, P., Kobayashi, S., Andrae, U., Balmaseda, M. A., Balsamo, G., Bauer, P., Bechtold, P., Beljaars, A. C. M., van de Berg, L., Bidlot, J., Bormann, N., Delsol, C., Dragani, R., Fuentes, M., Geer, A. J., … Vitart, F. (2011). The ERA-interim reanalysis: Configuration and performance of the data assimilation system. *Quarterly Journal of the Royal Meteorological Society*, 137(656), 553–597. https://doi.org/10.1002/qj.828

D'Odorico, P., & Porporato, A. (2004). Preferential states in soil moisture and climate dynamics. *Proceedings of the National Academy of Sciences*, 101(24), 8848–8851. https://doi.org/10.1073/pnas.0401428101

Done, J. M., Craig, G. C., Gray, S. L., Clark, P. A., & Gray, M. E. B. (2006). Mesoscale simulations of organized convection: Importance of convective equilibrium. *Quarterly Journal of the Royal Meteorological Society*, 132(616), 737–756. https://doi.org/10.1256/qj.04.84

Doswell, C. A., & Rasmussen, E. N. (1994). The effect of neglecting the virtual temperature correction on CAPE calculations. *Weather and Forecasting*, 9(4), 625–629. https://doi.org/10.1175/1520-0434(1994)009<0625:TEONTV>2.0.CO;2

Duerinck, H. M., van der Ent, R. J., van de Giesen, N. C., Schoups, G., Babovic, V., & Yeh, P. J.-F. (2016). Observed soil moisture–precipitation feedback in Illinois: A systematic analysis over different scales. *Journal of Hydrometeorology*, 17(6), 1645–1660. https://doi.org/10.1175/JHM-D-15-0032.1

Ek, M. B., & Holtslag, A. A. M. (2004). Influence of soil moisture on boundary layer cloud development. *Journal of Hydrometeorology*, 5(1), 86–99. https://doi.org/10.1175/1525-7541(2004)005<0086:IOSMOB>2.0.CO;2

Eltahir, E. A. B., & Bras, R. L. (1994). Precipitation recycling in the Amazon basin. *Quarterly Journal of the Royal Meteorological Society*, 120(518), 861–880. https://doi.org/10.1002/qj.49712051806

Fersch, B., Senatore, A., Adler, B., Arnault, J., Mauder, M., Schneider, K., Völksch, I., & Kunstmann, H. (2020). High-resolution fully coupled atmospheric–hydrological modeling: A cross-compartment regional water and energy cycle evaluation. *Hydrology and Earth System Sciences*, 24(5), 2457–2481. https://doi.org/10.5194/hess-24-2457-2020

Findell, K. L., & Eltahir, E. A. B. (1997). An analysis of the soil moisture-rainfall feedback, based on direct observations from Illinois. *Water Resources Research*, 33(4), 725–735. https://doi.org/10.1029/96WR03756

Findell, K. L., Gentine, P., Lintner, B. R., & Kerr, C. (2011). Probability of afternoon precipitation in eastern United States and Mexico enhanced by high evaporation. *Nature Geoscience*, 4(7), 434–439. https://doi.org/10.1038/ngeo1174

Froidevaux, P., Schlemmer, L., Schmidli, J., Langhans, W., & Schär, C. (2014). Influence of the background wind on the local soil moisture–precipitation feedback. *Journal of the Atmospheric Sciences*, 71(2), 782–799. https://doi.org/10.1175/JAS-D-13-0180.1

Funk, C., Peterson, P., Landsfeld, M., Pedreros, D., Verdin, J., Shukla, S., Husak, G., Rowland, J., Harrison, L., Hoell, A., & Michaelsen, J. (2015). The climate hazards infrared precipitation with stations—A new environmental record for monitoring extremes. *Scientific Data*, 2, 1–21. https://doi.org/10.1038/sdata.2015.66

Gartzke, J., Knuteson, R., Przybyl, G., Ackerman, S., & Revercomb, H. (2017). Comparison of satellite-, model-, and Radiosonde-derived convective available potential energy in the southern Great Plains region. *Journal of Applied Meteorology and Climatology*, 56(5), 1499–1513. https://doi.org/10.1175/JAMC-D-16-0267.1

Gentine, P., Massmann, A., Lintner, B. R., Hamed Alemohammad, S., Fu, R., Green, J. K., Kennedy, D., & Vilà-Guerau de Arellano, J. (2019). Land–atmosphere interactions in the tropics – A review. *Hydrology and Earth System Sciences*, 23(10), 4171–4197. https://doi.org/10.5194/hess-23-4171-2019

Gochis, D. J., Yu, W., & Yates, D. N. (2013). The WRF-Hydro Model Technical Description and User's Guide, Version 1.0, NCAR Technical Document. NCAR, Boulder, Colorado. https://ral.ucar.edu/projects/wrf_hydro/overview

Guillod, B. P., Orlowsky, B., Miralles, D. G., Teuling, A. J., & Seneviratne, S. I. (2015). Reconciling spatial and temporal soil moisture

effects on afternoon rainfall. *Nature Communications*, 6, 6443. https://doi.org/10.1038/ncomms7443

Hao, Z., Singh, V. P., & Xia, Y. (2018). Seasonal drought prediction: Advances, challenges, and future prospects. *Reviews of Geophysics*, 56(1), 108–141. https://doi.org/10.1002/2016RG000549

Hohenegger, C., Brockhaus, P., Bretherton, C. S., & Schär, C. (2009). The soil moisture–precipitation feedback in simulations with explicit and parameterized convection. *Journal of Climate*, 22(19), 5003–5020. https://doi.org/10.1175/2009JCLI2604.1

Hsu, H., Lo, M.-H., Guillod, B. P., Miralles, D. G., & Kumar, S. (2017). Relation between precipitation location and antecedent/subsequent soil moisture spatial patterns. *Journal of Geophysical Research: Atmospheres*, 122(12), 6319–6328. https://doi.org/10.1002/2016JD026042

Imamovic, A., Schlemmer, L., & Schär, C. (2017). Collective impacts of orography and soil moisture on the soil moisture-precipitation feedback. *Geophysical Research Letters*, 44(22), 11,682–11,691. https://doi.org/10.1002/2017GL075657

Keil, C., & Craig, G. C. (2011). Regime-dependent forecast uncertainty of convective precipitation. *Meteorologische Zeitschrift*, 20, 145–151. https://doi.org/10.1127/0941-2948/2011/0219

Keil, C., Heinlein, F., & Craig, G. C. (2014). The convective adjustment time-scale as indicator of predictability of convective precipitation. *Quarterly Journal of the Royal Meteorological Society*, 140(679), 480–490. https://doi.org/10.1002/qj.2143

Kerandi, N., Arnault, J., Laux, P., Wagner, S., Kitheka, J., & Kunstmann, H. (2018). Joint atmospheric-terrestrial water balances for East Africa: A WRF-hydro case study for the upper Tana River basin. *Theoretical and Applied Climatology*, 131(3), 1337–1355. https://doi.org/10.1007/s00704-017-2050-8

Kiese, R., Fersch, B., Baessler, C., Brosy, C., Butterbach-Bahl, K., Chwala, C., Dannenmann, M., Fu, J., Gasche, R., Grote, R., Jahn, C., Klatt, J., Kunstmann, H., Mauder, M., Rödiger, T., Smiatek, G., Soltani, M., Steinbrecher, R., Völksch, I., ... Schmid, H. P. (2018). The TERENO pre-alpine observatory: Integrating meteorological, hydrological, and biogeochemical measurements and modeling. *Vadose Zone Journal*, 17(1), 180060. https://doi.org/10.2136/vzj2018.03.0060

Korres, W., Reichenau, T. G., Fiener, P., Koyama, C. N., Bogena, H. R., Cornelissen, T., Baatz, R., Herbst, M., Diekkrüger, B., Vereecken, H., & Schneider, K. (2015). Spatio-temporal soil moisture patterns – A meta-analysis using plot to catchment scale data. *Journal of Hydrology*, 520, 326–341. https://doi.org/10.1016/j.jhydrol.2014.11.042

Koster, R. D., Dirmeyer, P. A., Guo, Z., Bonan, G., Chan, E., Cox, P., Gordon, C. T., Kanae, S., Kowalczyk, E., Lawrence, D., Liu, P., Lu, C.-H., Malyshev, S., McAvaney, B., Mitchell, K., Mocko, D., Oki, T., Oleson, K., Pitman, A., ... Yamada, T. (2004). Regions of strong coupling between soil moisture and precipitation. *Science*, 305(5687), 1138–1140. https://doi.org/10.1126/science.1100217

Koster, R. D., Sud, Y. C., Guo, Z., Dirmeyer, P. A., Bonan, G., Oleson, K. W., Chan, E., Verseghy, D., Cox, P., Davies, H., Kowalczyk, E., Gordon, C. T., Kanae, S., Lawrence, D., Liu, P., Mocko, D., Lu, C.-H., Mitchell, K., Malyshev, S., ... Xue, Y. (2006). GLACE: The global land–atmosphere coupling experiment. Part I: Overview. *Journal of Hydrometeorology*, 7(4), 590–610. https://doi.org/10.1175/JHM510.1

Krishnamurti, T. N. (1968). A calculation of percentage area covered by convective clouds from moisture convergence. *Journal of Applied Meteorology*, 7(2), 184–195. https://doi.org/10.1175/1520-0450(1968)007<0184:ACOPAC>2.0.CO;2

Kühnlein, C., Keil, C., Craig, G. C., & Gebhardt, C. (2014). The impact of downscaled initial condition perturbations on convective-scale ensemble forecasts of precipitation. *Quarterly Journal of the Royal Meteorological Society*, 140(682), 1552–1562. https://doi.org/10.1002/qj.2238

Kunstmann, H., & Jung, G. (2007). Influence of soil-moisture and land use change on precipitation in the Volta Basin of West Africa. *International Journal of River Basin Management*, 5(1), 9–16. https://doi.org/10.1080/15715124.2007.9635301

Larsen, M. A. D., Christensen, J. H., Drews, M., Butts, M. B., & Refsgaard, J. C. (2016). Local control on precipitation in a fully coupled climate-hydrology model. *Scientific Reports*, 6(1), 22927. https://doi.org/10.1038/srep22927

Leutwyler, D., Imamovic, A., & Schär, C. (2021). The continental-scale soil moisture–precipitation feedback in Europe with parameterized and explicit convection. *Journal of Climate*, 34(13), 5303–5320. https://doi.org/10.1175/JCLI-D-20-0415.1

Liu, D., Yu, Z., & Mishra, A. K. (2017). Evaluation of soil moisture-precipitation feedback at different time scales over Asia. *International Journal of Climatology*, 37(9), 3619–3629. https://doi.org/10.1002/joc.4943

Maxwell, R. M., Chow, F. K., & Kollet, S. J. (2007). The groundwater–land-surface–atmosphere connection: Soil moisture effects on the atmospheric boundary layer in fully-coupled simulations. *Advances in Water Resources*, 30(12), 2447–2466. https://doi.org/10.1016/j.advwatres.2007.05.018

Niu, G.-Y., Yang, Z.-L., Mitchell, K. E., Chen, F., Ek, M. B., Barlage, M., Kumar, A., Manning, K., Niyogi, D., Rosero, E., Tewari, M., & Xia, Y. (2011). The community Noah land surface model with multiparameterization options (Noah-MP): 1. Model description and evaluation with local-scale measurements. *Journal of Geophysical Research: Atmospheres*, 116(D12), 1–19. https://doi.org/10.1029/2010JD015139

Notaro, M. (2008). Statistical identification of global hot spots in soil moisture feedbacks among IPCC AR4 models. *Journal of Geophysical Research: Atmospheres*, 113(D9), 1–8. https://doi.org/10.1029/2007JD009199

Petersen, R. A., & Petersen, R. A. (2000, September 16). An analysis of low-level moisture flux convergence prior to the 3 May 1999 Oklahoma City tornadoes. Orlando Meeting. https://ams.confex.com/ams/Sept2000/webprogram/Paper16177.html

Powers, J. G., Klemp, J. B., Skamarock, W. C., Davis, C. A., Dudhia, J., Gill, D. O., Coen, J. L., Gochis, D. J., Ahmadov, R., Peckham, S. E., Grell, G. A., Michalakes, J., Trahan, S., Benjamin, S. G., Alexander, C. R., Dimego, G. J., Wang, W., Schwartz, C. S., Romine, G. S., ... Duda, M. G. (2017). The weather research and forecasting model: Overview, system efforts, and future directions. *Bulletin of the American Meteorological Society*, 98(8), 1717–1737. https://doi.org/10.1175/BAMS-D-15-00308.1

Rahman, M., Sulis, M., & Kollet, S. J. (2015). The subsurface–land surface–atmosphere connection under convective conditions. *Advances in Water Resources*, 83, 240–249. https://doi.org/10.1016/j.advwatres.2015.06.003

Rauthe, M., Steiner, H., Riediger, U., Mazurkiewicz, A., & Gratzki, A. (2013). A central European precipitation climatology – Part I: Generation and validation of a high-resolution gridded daily data set (HYRAS). *Meteorologische Zeitschrift*, 22, 235–256. https://doi.org/10.1127/0941-2948/2013/0436

Rieck, M., Hohenegger, C., & van Heerwaarden, C. C. (2014). The influence of land surface heterogeneities on cloud size development. *Monthly Weather Review*, 142(10), 3830–3846. https://doi.org/10.1175/MWR-D-13-00354.1

Riemann-Campe, K., Fraedrich, K., & Lunkeit, F. (2009). Global climatology of convective available potential energy (CAPE) and convective inhibition (CIN) in ERA-40 reanalysis. *Atmospheric Research*, 93(1), 534–545. https://doi.org/10.1016/j.atmosres.2008.09.037

Rummler, T., Arnault, J., Gochis, D., & Kunstmann, H. (2019). Role of lateral terrestrial water flow on the regional water cycle in a complex terrain region: Investigation with a fully coupled model system. *Journal of Geophysical Research: Atmospheres*, 124(2), 507–529. https://doi.org/10.1029/2018JD029004

Santanello, J. A., Dirmeyer, P. A., Ferguson, C. R., Findell, K. L., Tawfik, A. B., Berg, A., Ek, M., Gentine, P., Guillod, B. P., van Heerwaarden, C., Roundy, J., & Wulfmeyer, V. (2018). Land–

atmosphere interactions: The LoCo perspective. *Bulletin of the American Meteorological Society*, *99*(6), 1253–1272. https://doi.org/10.1175/BAMS-D-17-0001.1

Santanello, J. A., Kumar, S. V., Peters-Lidard, C. D., & Lawston, P. M. (2016). Impact of soil moisture assimilation on land surface model Spinup and coupled land–atmosphere prediction. *Journal of Hydrometeorology*, *17*(2), 517–540. https://doi.org/10.1175/JHM-D-15-0072.1

Senatore, A., Mendicino, G., Gochis, D. J., Yu, W., Yates, D. N., & Kunstmann, H. (2015). Fully coupled atmosphere-hydrology simulations for the Central Mediterranean: Impact of enhanced hydrological parameterization for short and long time scales. *Journal of Advances in Modeling Earth Systems*, *7*(4), 1693–1715. https://doi.org/10.1002/2015MS000510

Seneviratne, S. I., Corti, T., Davin, E. L., Hirschi, M., Jaeger, E. B., Lehner, I., Orlowsky, B., & Teuling, A. J. (2010). Investigating soil moisture–climate interactions in a changing climate: A review. *Earth-Science Reviews*, *99*(3), 125–161. https://doi.org/10.1016/j.earscirev.2010.02.004

Skamarock, W. C., Klemp, J. B., Dudhia, J., Gill, D. O., Barker, D. M., Wang, W., & Powers, J. G. (2005). A description of the advanced research WRF version 2. NCAR Tech. Note.

Su, H., & Dickinson, R. E. (2017). On the spatial gradient of soil moisture–precipitation feedback strength in the April 2011 drought in the southern Great Plains. *Journal of Climate*, *30*(3), 829–848. https://doi.org/10.1175/JCLI-D-13-00185.1

Taylor, C. M., Birch, C. E., Parker, D. J., Dixon, N., Guichard, F., Nikulin, G., & Lister, G. M. S. (2013). Modeling soil moisture-precipitation feedback in the Sahel: Importance of spatial scale versus convective parameterization. *Geophysical Research Letters*, *40*(23), 6213–6218. https://doi.org/10.1002/2013GL058511

Taylor, C. M., de Jeu, R. A. M., Guichard, F., Harris, P. P., & Dorigo, W. A. (2012). Afternoon rain more likely over drier soils. *Nature*, *489*(7416), 423–426. https://doi.org/10.1038/nature11377

Taylor, C. M., Gounou, A., Guichard, F., Harris, P. P., Ellis, R. J., Couvreux, F., & De Kauwe, M. (2011). Frequency of Sahelian storm initiation enhanced over mesoscale soil-moisture patterns. *Nature Geoscience*, *4*(7), 430–433. https://doi.org/10.1038/ngeo1173

Taylor, C. M., & Lebel, T. (1998). Observational evidence of persistent convective-scale rainfall patterns. *Monthly Weather Review*, *126*(6), 1597–1607. https://doi.org/10.1175/1520-0493(1998)126<1597:OEOPCS>2.0.CO;2

van der Ent, R. J., & Savenije, H. H. G. (2011). Length and time scales of atmospheric moisture recycling. *Atmospheric Chemistry & Physics*, *11*, 1853–1863. https://doi.org/10.5194/acp-11-1853-2011

van Zomeren, J., & van Delden, A. (2007). Vertically integrated moisture flux convergence as a predictor of thunderstorms. *Atmospheric Research*, *83*(2), 435–445. https://doi.org/10.1016/j.atmosres.2005.08.015

Wei, J., Su, H., & Yang, Z.-L. (2016). Impact of moisture flux convergence and soil moisture on precipitation: A case study for the southern United States with implications for the globe. *Climate Dynamics*, *46*(1), 467–481. https://doi.org/10.1007/s00382-015-2593-2

Wolf, B., Chwala, C., Fersch, B., Garvelmann, J., Junkermann, W., Zeeman, M. J., Angerer, A., Adler, B., Beck, C., Brosy, C., Brugger, P., Emeis, S., Dannenmann, M., De Roo, F., Diaz-Pines, E., Haas, E., Hagen, M., Hajnsek, I., Jacobeit, J., … Schmid, H. P. (2017). The SCALEX campaign: Scale-crossing land surface and boundary layer processes in the TERENO-preAlpine observatory. *Bulletin of the American Meteorological Society*, *98*(6), 1217–1234. https://doi.org/10.1175/BAMS-D-15-00277.1

Yang, L., Sun, G., Zhi, L., & Zhao, J. (2018). Negative soil moisture-precipitation feedback in dry and wet regions. *Scientific Reports*, *8*, 4026. https://doi.org/10.1038/s41598-018-22394-7

Yin, J., Albertson, J. D., Rigby, J. R., & Porporato, A. (2015). Land and atmospheric controls on initiation and intensity of moist convection: CAPE dynamics and LCL crossings. *Water Resources Research*, *51*(10), 8476–8493. https://doi.org/10.1002/2015WR017286

Zaitchik, B. F., Santanello, J. A., Kumar, S. V., & Peters-Lidard, C. D. (2013). Representation of soil moisture feedbacks during drought in NASA unified WRF (NU-WRF). *Journal of Hydrometeorology*, *14*(1), 360–367. https://doi.org/10.1175/JHM-D-12-069.1